GENERATION AND DETECTION OF ACOUSTIC WAVEGUIDE MODES IN ULTRATHIN CRYSTALS USING THE TRANSIENT GRATING TECHNIQUE

Jeffrey S. METH, C.D. MARSHALL and M.D. FAYER
Department of Chemistry, Stanford University, Stanford, CA 94305, USA

Received 30 June 1989; in final form 10 August 1989

The generation of acoustic waveguide modes (Lamb waves) in ultrathin solids using the transient grating (TG) technique is described. The driving force due to the TG excitation is derived for a free, isotropic plate. In contrast to a bulk isotropic material in which a single wave is excited, the TG excites a number of modes with a variety of frequencies but with the same wavevector. The frequencies beat, resulting in a complex time-dependent signal. Experimental results for anthracene sublimation flakes of ≈ 1 μm thicknesses are presented. Lamb waves with frequencies that do not match the bulk frequencies are generated.

1. Introduction

The mechanical degrees of freedom of a solid play a central role in determining material properties. Phonon spectra of solids provide information about mechanical properties and intermolecular interactions. The scattering and attenuation of acoustic phonons can be used to investigate strains and defects in a solid [1]. Recently there has been considerable interest in ultrathin (<1 μm) materials in electronics [2], coatings [3], optics [4], and other areas. To investigate ultrathin materials it is necessary to generate and detect a variety of ultrasonic wave frequencies and wavevectors in a situation which is not readily amenable to conventional acoustic wave methods [1] which involve contacting transducers to the sample. Here we report an optical holographic method (transient grating) [5] for the generation and detection of acoustic waveguide modes (Lamb waves [6]) in ultrathin materials such as crystals and films. The transient grating (TG) method does not require mechanical contact with the sample, and therefore can be applied to delicate materials.

The coherent generation and detection of phonons in bulk condensed matter systems using the TG technique has been described in detail previously [5]. In the TG experiment (fig. 1), two picosecond laser pulses are overlapped spatially and temporally in a sample. The interference between the two pulses of wavelength λ creates a fringe pattern in the sample where the fringe spacing d is related to the angle between the beams, θ, by the relation

$$d=\tfrac{1}{2}\lambda \sin \tfrac{1}{2}\theta=2\pi/\beta\,. \qquad (1)$$

The electromagnetic energy in the interference pattern couples to the sample, creating acoustic waves [5]. The wavelength of the acoustic waves is determined by the fringe spacing. The induced acoustic waves (density waves) produce a time-dependent

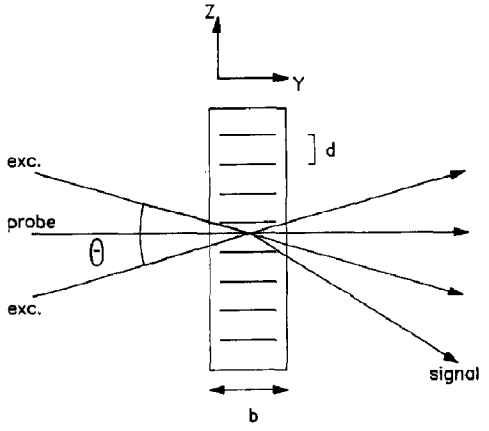

Fig. 1. The transient grating set-up. θ is the crossing angle of the beams, b is the thickness of the sample, and d is the fringe spacing.

0 009-2614/89/$ 03.50

modulation of the sample's density, and hence generate a time-dependent oscillation in the real part of the index of refraction of the medium. The time-dependent oscillation of the index of refraction spatially mimics the optical interference pattern and acts as a Bragg diffraction grating. A third, variably-time delayed, picosecond pulse diffracts from the induced acoustic wave grating. The diffracted signal beam intensity reflects the magnitude and the time dependence of the optically induced density waves.

TG-acoustic wave experiments on waveguides are fundamentally different from the analogous experiments conducted on thick samples. Until now, this technique has only been applied to bulk samples, where a single wave is generated in an isotropic material or when the grating is aligned along a rotational symmetry axis of a crystal. In this Letter, we present a treatment of the phenomenon that is applicable to acoustic waveguides, and we demonstrate that a superposition of acoustic waves with many different frequencies is generated. The phase velocities of the waveguide modes will not necessarily match those of the bulk material. In addition, the spatial structure of the waveguide modes influences the nature of the detection of the waves as well as the generation.

In a waveguide it is necessary to take into account the effects of the surfaces [6]. For a thin plate surrounded by vacuum (z is the grating direction and y is the perpendicular to the plane), the acoustic waves are reflected by the surfaces. At a surface, the longitudinal waves (compressional, k vector parallel to the polarization vector) couple with the shear waves polarized in the yz plane. Thus the normal modes in the waveguide are combinations of shear and longitudinal waves [6]. For a normal mode, the motion of a microscopic volume element is elliptical. The axes of the ellipse are parallel and perpendicular to the plate surfaces, and the eccentricity of the ellipse varies with the normal mode. These normal modes are known as Lamb modes [6], and can be separated into two families, symmetric and antisymmetric, depending on the symmetry of the velocity fields when reflected in the xz plane (see fig. 2).

In the material presented below, we briefly describe the theory of the generation of Lamb modes in a free, isotropic plate for the initial conditions created by the TG technique. We also present TG experiments performed on ultrathin anthracene sublimation flakes with the grating directed along the b axis, which is a twofold screw axis. Unlike the case of a bulk sample, where only one acoustic wave is generated, we demonstrate that many waves with different frequencies are generated in the waveguide. This is a nonintuitive result with implications in the field of waveguide device design and nondestructive evaluation.

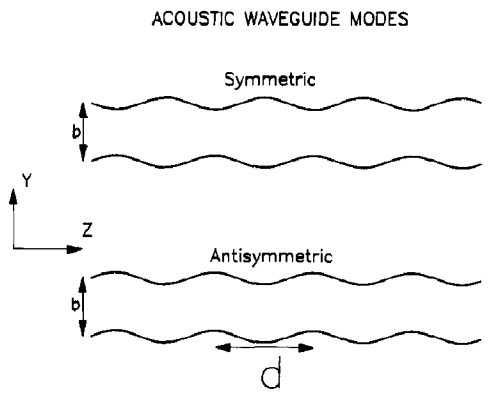

Fig. 2. Symmetric (dilatational) and antisymmetric (flexural) acoustic waveguide modes. d is the fringe spacing, b is the thickness. The modes are symmetric and antisymmetric with respect to reflection in the xz plane, the plane of the waveguide. x is out of the plane of the figure.

2. Experimental procedures

The experimental setup will be described in detail elsewhere [7]. Basically, a Q-switched, mode-locked Nd:YAG laser operating at 600 Hz repetition rate is used to synchronously pump two cavity-dumped dye lasers. One of the 1.06 μm pulses is selected and summed with the cavity-dumped pulse from one of the dye lasers to provide a tunable source of near UV, 30 ps, 3 μJ pulses. The other dye laser is cavity dumped to provide a tunable probe wavelength in the red with similar pulse duration and energy. In some experiments both the excitation and probe wavelengths were in the UV.

The diffracted signals were detected in transmission. Because the samples are very thin the Bragg diffraction condition is relaxed. The probe is brought

in normal to the sample, and it bisects the angle made by the excitation beams.

The signal is detected with a photomultiplier and a lock-in amplifier. A motorized delay line scans the delay between the probe pulse and the excitation pulses. A computer digitizes the signal intensity and a voltage which is proportional to the probe pulse delay, then averages several scans of the delay line to improve the signal to noise ratio.

3. Theory

To understand the nature of the acoustic disturbance created in a thin plate by TG excitation, it is necessary to determine the driving force created by the optical interference pattern. We consider undamped and damped (to account for absorption) electromagnetic fields. The driving force excites a superposition of Lamb waves. By knowing the amplitude and frequency of these waves, it is possible to calculate the time-dependent intensity of the signal which is diffracted from the acoustic wave phase grating.

The wavevector dependence of the Lamb mode frequencies was calculated using the dispersion relations for a free, isotropic plate [6]. This was done numerically, and the results are displayed graphically in fig. 3a for the symmetric modes and in fig. 3b for the antisymmetric modes. The calculations employed constants appropriate for an anthracene single crystal, but treated it as isotropic. The plane of the plate corresponds to the anthracene *ab* plane. While it is possible to do the calculations for the actual anisotropic solid, the complexity of the calculation is vastly magnified. Notice that the axes are scaled by b, the thickness of the waveguide. Scaled in this manner, the dispersion relations have the same shape for any sample thickness. The spatial dependences of the velocity fields of the Lamb modes are given by

$$v_y = \{-k_{t\ell} \sin k_{t\ell} y \cos \tfrac{1}{2} k_{ts} b - [(\beta^2 - k_{ts}^2)/2k_{ts}] \cos \tfrac{1}{2} k_{t\ell} b \sin k_{ts} y\} \times \exp(\mp i\beta z), \quad (2a)$$

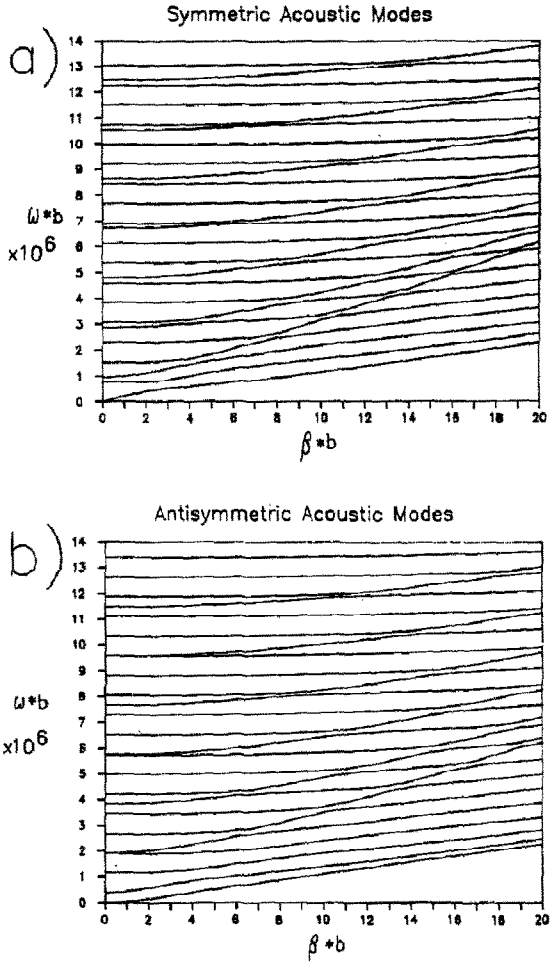

Fig. 3. Dispersion relations for a free, isotropic plate waveguide. (a) Symmetric Lamb modes. (b) Antisymmetric Lamb modes. The calculations were performed using constants for an anthracene crystal modeled as isotropic.

$$v_z = \mp i\beta\{\cos k_{t\ell} y \cos \tfrac{1}{2} k_{ts} b - [(\beta^2 - k_{ts}^2)/2\beta^2] \cos \tfrac{1}{2} k_{t\ell} b \cos k_{ts} y\} \times \exp(\mp i\beta z), \quad (2b)$$

for the symmetric modes, and

$$v_y = \{k_{t\ell} \cos k_{t\ell} y \sin \tfrac{1}{2} k_{ts} b + [(\beta^2 - k_{ts}^2)/2k_{ts}] \sin \tfrac{1}{2} k_{t\ell} b \cos k_{ts} y\} \times \exp(\mp i\beta z), \quad (3a)$$

$$v_z = \mp i\beta\{\sin k_{t\ell} y \sin \tfrac{1}{2} k_{ts} b - [(\beta^2 - k_{ts}^2)/2\beta^2] \sin \tfrac{1}{2} k_{t\ell} b \sin k_{ts} y\} \times \exp(\mp i\beta z) \quad (3b)$$

for the antisymmetric modes. In the above equations, $k_{t\ell}$ and k_{ts} are the transverse components of the longitudinal and shear partial waves and are related to β and ω by the formulae [6]

$$\beta^2 + k_{t\ell}^2 = \omega^2 / V_\ell^2 , \quad (4a)$$

$$\beta^2 + k_{ts}^2 = \omega^2 / V_s^2 , \quad (4b)$$

where V_ℓ and V_s are the longitudinal and shear velocities, respectively.

The superposition of normal modes can be written as

$$\sum a_m \phi_m(y, z) + \sum b_n \psi_n(y, z) = G(y, z) , \quad (5)$$

where ϕ refers to the symmetric modes and ψ refers to the antisymmetric modes. The quantity G specifies the driving force for a certain k vector, not for a particular frequency.

Unlike a transducer, which drives the system at a specific frequency (along a horizontal line in figs. 3a or 3b), the TG drives a system at a given wavevector (along a vertical line in figs. 3a or 3b). This is a fundamental difference between mechanical and optical excitation of a waveguide. In a bulk sample, where there is only one frequency associated with the grating wavevector, that mode is excited. In a waveguide many different frequencies will be simultaneously generated and observed.

To solve for the amplitudes a, b, one multiplies eq. (5) by a normal mode then integrates. If the modes were orthogonal to one another, all cross products between the modes would equal zero. Although Lamb modes at the same frequency but different wavevectors are orthogonal to one another, this is not the case when the different modes have the same wavevector but different frequencies. Since the modes excited by the TG are not orthogonal, one obtains a matrix representing the overlap between different modes:

$$\Phi_{jk} = \int\int \phi_j \phi_k \, dy \, dz , \quad (6a)$$

$$\Psi_{jk} = \int\int \psi_j \psi_k \, dy \, dz . \quad (6b)$$

By representing the driving force as a sum of symmetric and anitsymmetric forces, and using the fact that the symmetric Lamb modes are always orthogonal to the antisymmetric modes, one arrives at the following two matrix equations which need to be inverted,

$$\Phi \cdot A = G_s , \quad (7a)$$

$$\Psi \cdot B = G_a . \quad (7b)$$

Here, A and B are column vectors representing the amplitudes of the coefficients of the Lamb waves. These equations are inverted numerically to yield the amplitudes of the Lamb waves that are generated.

There are two mechanisms [8] by which the TG technique generates a driving force to launch acoustic waves: heating by rapid radiationless relaxation following optical absorption [9] and stimulated Brillouin scattering [10]. The heating mechanism is responsible for acoustic wave formation in the data presented here [7]. For a single wave, the strain has a time dependence which is proportional to $1 - \cos(\omega t)$.

The spatial form of the driving force which excites the superposition of Lamb waves is

$$G_y = -\exp(-\alpha y)\{c_{11} P\alpha(2 - \alpha y) + \cos \beta z \times [c_{11} P\alpha(2 - \alpha y) + c_{12} Q\alpha\beta + c_{44}\beta(Q\alpha + P\beta y)]\} , \quad (8a)$$

$$G_z = \exp(-\alpha y) \sin \beta z \times \{c_{44}[P\alpha^2 - Q\beta(1 - \alpha y)] - c_{12}\beta Q(1 - \alpha y) - c_{11}\beta^2 P\} , \quad (8b)$$

where P, Q are constants, c_{ij} are elastic constants, and α is the absorption coefficient of the sample.

One can understand the origin of this driving force in the following manner [8]. At time $t = 0$, the sample has been excited by the driving force but there are no displacements. The total strain, $S = 0$. The strain induced by thermal expansion in the grating peaks is identically cancelled by the acoustic strain at $t = 0$. One solves for the thermal strain and then calculates the stress due to that strain. The gradient of the calculated stress is equal to the negative of the driving force applied at $t = 0$. The thermal strain along z (the direction of the grating) is identical to that of the bulk case [8]. In the y direction, however, there

is no restoring force to counter thermal expansion. Thermal expansion corrugates the surfaces of the crystal, creating the differences between the waveguide driving force and the driving force in a bulk sample.

From the theory several basic features of TG excitation of wave guides can be discerned. First, if one uses a driving force which is not damped (the optical field is not attentuated passing through the sample), only symmetric modes are excited. This is because the driving force is symmetric with respect to the mirror plane xz. Conversely, if the driving force is damped (optical absorption) both symmetric and antisymmetric modes are excited. Second, the use of perpendicularly polarized pulses will generate vertically polarized (x-polarized) shear waves in analogy to the generation of shear waves in bulk materials [11]. Shear wave generation has not yet been demonstrated.

4. Results and discussion

In general, the theory predicts that modes with phase velocities ω/β less than that of the bulk longitudinal mode will be mainly excited. When the outer diameter is sufficiently low (<0.5) chiefly symmetric modes are generated. When the outer diameter becomes greater, antisymmetric modes are also created. The lowest symmetric (S_1) and antisymmetric (A_1) modes have substantial amplitude in all cases, although A_1 is not always observed due to the intricacies of the detection mechanism [7]. These two modes combine at large (>8) values of βb to produce the Rayleigh wave [6]. In the experiments presented here, βb lies between 0 and 5. In general, one excites, and expects to observe, a combination of acoustic waves with different frequencies that beat against one another.

This is demonstrated in fig. 4, which displays the TG response of an anthracene flake. The exciting and probing frequencies of the grating are degenerate and polarized along the a axis. Their wavelength is 378 nm, where the outer diameter $=0.45$ for this crystal, which is 0.6 μm thick. The grating points along the b axis with $d=2.9$ μm. In this case $\beta b=1.3$. The fast Fourier transform (FFT) of this data set reveals three frequencies, with phase velocities $\omega/\beta=2.25\times10^5$, $\omega/\beta=4.83\times10^5$, and $\omega/\beta=7.40\times10^5$ cm/s. Notice that none of the frequencies corresponds to the bulk frequency along the b axis; 2.80×10^5 cm/s reported recently by Dye and Eckhardt [12] or the slightly greater frequency 3×10^5 cm/s given in older studies [13]. The isotropic model predicts that the first three symmetric Lamb waves will be observed and that they have frequencies of $\omega/\beta=2.16\times10^5$, $\omega/\beta=5.80\times10^5$, $\omega/\beta=8.06\times10^5$. This is in reasonable

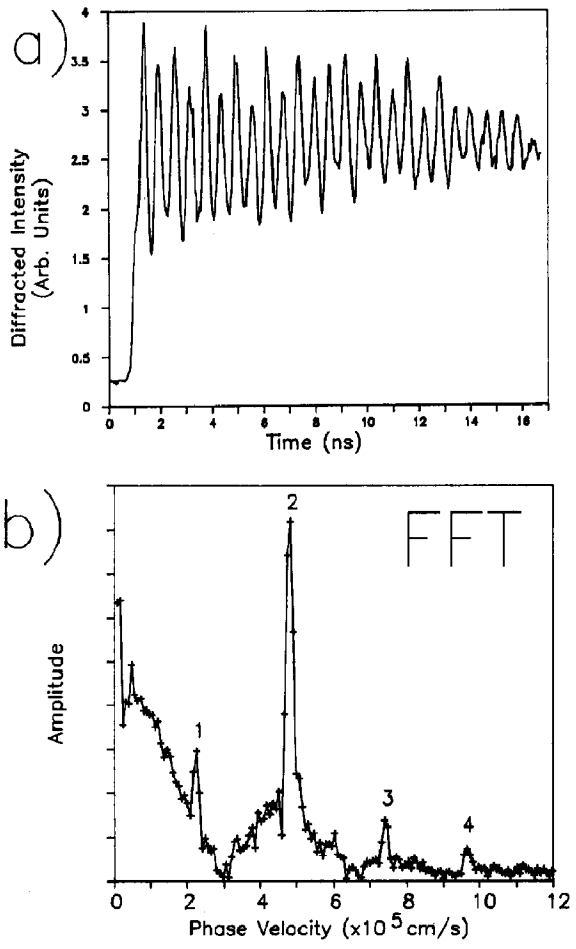

Fig. 4. Transient grating response of a 0.6 μm thick anthracene sublimation flake. Excitation and probe beams have a wavelength $\lambda=378$ nm, and are a-polarized. The grating is directed along the b axis of the crystal and $d=2.9$ μm. (a) Time domain response illustrating the characteristic beating pattern. (b) FFT clearly shows three peaks: peak 1 at $\omega/\beta=2.25\times10^5$ cm/s, peak 2 at $\omega/\beta=4.83\times10^5$ cm/s, and peak 3 at $\omega/\beta=7.40\times10^5$ cm/s. Peak 4 is the second harmonic of 2 and is an artifact of the FFT procedure. The structure near $\omega=0$ is caused by the constant offset in the time domain.

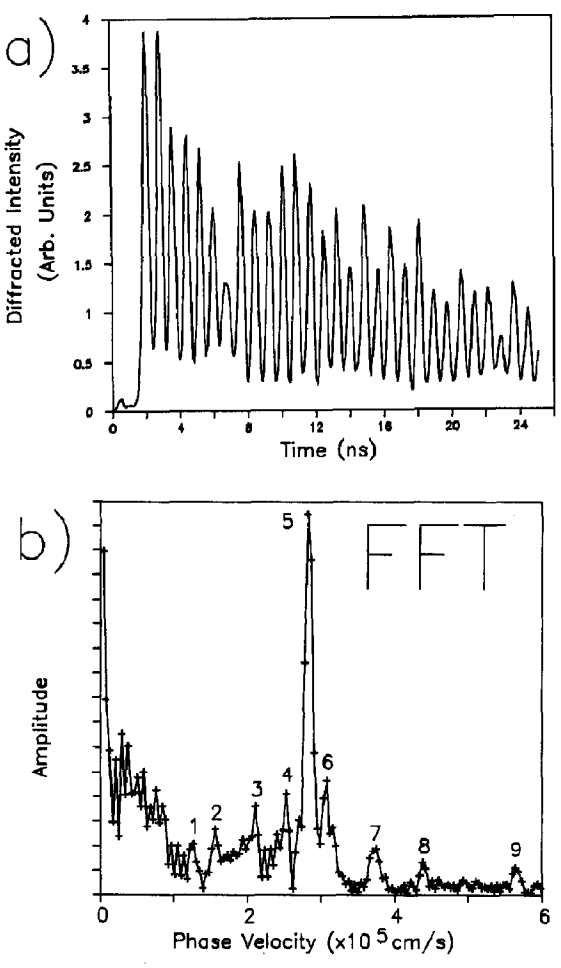

Fig. 5. Transient grating response of an anthracene sublimation flake in the high outer diameter regime. Excitation beams have a wavelength $\lambda=398$ nm, and are b-polarized; the probe beam has a wavelength $\lambda=624$ nm, and is b-polarized. The grating is directed along the crystallographic b axis and $d=2.28$ μm. (a) Time domain response showing mainly one frequency. (b) FFT of the data shows that eight modes are excited. The main frequency at peak 5 corresponds to $\omega/\beta=2.82\times10^5$ cm/s. Peak 9 is the second harmonic of peak 5. Again, the structure near $\omega=0$ is caused by the constant offset in the time domain.

agreement with the data considering that the anisotropic nature of the anthracene crystal is not included in the model.

Data from a high outer diameter sample is displayed in fig. 5. The data were taken with the two exciting beams at 398 nm, b-polarized, and the probe beam at 624 nm, b-polarized. The grating is aligned along the b axis with $d=2.28$ μm so that βb is about 5. To the eye, there is clearly a dominant frequency and a complex beating pattern. All of the features in the data are reproducible. In addition to the dominant frequency the FFT of the data reveals seven other modes with significant amplitude. The dominant mode has a phase velocity of 2.82×10^5 cm/s, which is close to the bulk value reported by Dye and Eckhardt [12]. Table 1 compares the observed phase velocities with those predicted to have significant amplitude by the model.

The data presented in figs. 4 and 5 are consistent with the theory briefly described in section 3. Transient grating generation of acoustic waves in a waveguide is distinctly different from generation in a bulk sample. Multiple waveguide modes can be excited, and the phase velocities of these modes do not necessarily correspond to the bulk velocity. The frequencies which are excited are characteristic of the waveguide dispersion relations.

The fact that the strain due to a Lamb wave is not uniform in the y direction also influences the observed diffraction. In a bulk material, where this strain is uniform, it is not necessary to consider the nature of the perturbation of the dielectric tensor in a microscopic volume element because the probing electric field experiences the same perturbation throughout the sample. When multiple waves are excited in a bulk crystal (by aligning the grating along a non-symmetry direction) [5], the diffracted intensity is directly proportional to the amplitudes of the waves. In the waveguide, however, the spatial

Table 1
Calculated versus observed phase velocities for anthracene ($\times10^5$ cm/s)

	Mode								
	A_1	S_1	A_2	S_2	A_3	S_3	S_4	A_4	A_5
obs.	1.26	1.56	2.11	2.53	2.82	3.07	3.71	4.38	5.64
calc.	1.07	1.36	1.90	2.34	2.78	3.23	3.70	3.99	4.87

variation of the strain along the y direction necessitates consideration of the microscopic process of diffraction to determine the observed signal. Furthermore, the amplitudes of the frequency components in the diffracted signal are not simply related to the amplitudes of the Lamb waves in the sample. This effect is observed experimentally and will be described in detail in a future publication [7].

The theory presented is for an isotropic medium and is only approximately applicable to anthracene. The isotropic approximation is valid when the slowness curves [6] of anthracene can be approximated as circles. This approximation is valid when the ratio between the transverse component of the wavevector is small compared to β, the k vector of the grating. This is true for modes whose phase velocity is close to the phase velocity of the bulk and for surface waves. The agreement between experiment and theory presented in fig. 4 is a good example of this concept.

5. Concluding remarks

Extending optical acoustic wave generation from the bulk to ultrathin waveguide materials makes it possible to explore the nature of very thin media. A particular wavevector, not a particular frequency is excited. It is possible to obtain mechanical information without making physical contact to the sample. If the thickness of a sample is known, the dispersion relations for the material can be obtained by varying the fringe spacing. Conversely, if one knows the dispersion of a material, it is possible to measure the thickness using the transient grating technique. By focusing the optical beams to a small spot size, local environments can be probed, and local elastic constants can be measured.

Acknowledgement

The authors would like to thank the National Science Foundation Division of Materials Research (DMR 87-18959) for supporting this research.

References

[1] G.S. Kino, Science 206 (1979) 175; Acoustic waves (Prentice-Hall, Englewood Cliffs, 1987) ch. 3.
[2] C.M. Sotomayor Torres et al., Optical properties of narrow-gap low-dimensional structures (Plenum Press, New York, 1987).
[3] M. Munch, A. Gast, J. Chem. Soc. Faraday Trans. I, (1989), in press.
[4] G.I. Stegeman, R. Zanoni, K. Rochford and C.T. Seaton, in: Nonlinear optical effects in organic polymers, eds. J. Messier et al. (Plenum Press, New York, 1989) p. 257.
[5] M.D. Fayer, IEEE J. Quantum Electron QE-22 (1986) 1437.
[6] B.A. Auld, Acoustic fields and waves in solids, Vol. 2 (Wiley, New York, 1973) ch. 10.
[7] J.S. Meth, C.D. Marshall and M.D. Fayer, to be published (1990).
[8] K.A. Nelson, R.J.D. Miller, D.R. Lutz, M.D. Fayer, J. Appl. Phys. 53 (1982) 1144.
[9] K.A. Nelson, M.D. Fayer, J. Chem. Phys. 72 (1980) 5202.
[10] K.A. Nelson, D.R. Lutz, M.D. Fayer and L. Madison, Phys. Rev. B 24 (1981) 3261.
[11] K.A. Nelson, J. Appl. Phys. 53 (1982) 6060.
[12] R.C. Dye and C.J. Eckhardt, J. Chem. Phys. 90 (1989) 2090.
[13] B. Dorner, E.L. Boknenkov, S.L. Chaplot, J. Kalus, I. Natkaniec, G.S. Pawley, U. Schmelzer and E.F. Sheka, J. Phys. C 15 (1982) 2353;
H.B. Huntington, S.G. Gangoli and J.L. Mills, J. Chem. Phys. 50 (1969) 3844;
T. Danno and H. Inokuchi, Bull. Chem. Soc. Japan 41 (1968) 1783;
G.K. Afanaseva, K.S. Aleksandrov and A.I. Kitaigorodskii, Phys. Stat. Sol. 24 (1967) K61.